

Supplementary Information

Six cobalt(II), zinc(II), nickel(II) and copper(II) complexes based on bis-benzimidazolyl bidentate ligands with phenolyl ether linkers: synthesis, structural studies and recognition for HSO_4^-

Zhixiang Zhao,^a Yue Yang,^a Linhai Hu,^a Jianhua Wang,^a Jie Yu^a and Qingxiang Liu*^a

^a *Tianjin Key Laboratory of Structure and Performance for Functional Molecules, College of Chemistry, Tianjin Normal University, Tianjin 300387, P. R. China.*

* Corresponding author, E-mail: tjnulqx@163.com

Table of Contents

1. General procedures.
2. X-ray data collection and structure determinations.
3. CCDC numbers for complexes **1-6**.
4. Summary of crystallographic data for complexes **1-6** (Table S1-Table S2).
5. The data of hydrogen bonds, π - π interactions and C-H \cdots π contacts of complexes **1-6** (Table S3-Table S4).
6. The solid-state fluorescences of **L₁-L₃** and complexes **1-6** (Fig. S1-Fig. S3).
7. The simulated and the experimental PXRD patterns for complexes **1-6** (Fig. S4-Fig. S9).
8. The curves of thermogravimetric analysis for complexes **1-6** (Fig. S10-Fig. S15).
9. The Fig.s of fluorescence and UV/vis spectroscopies for complex **1** (Fig. S16-Fig. S23).
10. The Fig. of HRMS for **1·HSO₄⁻** (Fig. S24).
11. Infrared spectra of **1** and **1·HSO₄⁻** (Fig. S25).

1. General procedures

All solvents, reagents were purchased commercially and were not further purified before use. A Bruker AVANCE III spectrometer was used to record NMR spectra. HRMS was obtained on the mass spectrometer (A VG ZAB-HS). The elemental analyses were obtained by using a Perkin-Elmer 2400C Elemental Analyzer. IR spectra (KBr), fluorescence spectra and UV spectra were gotten by a Bruker Equinox 55 spectrometer, a RF-5301PC fluorescence spectrophotometer (Shimadzu) and a JASCO-V570 spectrometer, respectively. The elemental analyses were performed using a Perkin-Elmer 2400C Elemental Analyzer. The solid-state fluorescence spectra were obtained using a Fluorolog-3 fluorescence spectrophotometer from Horiba Jobin Yvon. The powder X-ray diffraction patterns were recorded using a D/Max-III A diffractometer with a Cu-target tube ($\lambda = 1.5418 \text{ \AA}$) and a graphite monochromator. Thermogravimetric analysis (TG) was performed in N_2 at a heating rate of $20 \text{ }^{\circ}\text{C min}^{-1}$ using a NETZSCH TG209F3.

2. X-ray data collection and structure determinations

A Bruker Apex II CCD diffractometer was utilized to collect diffraction data for complexes **1-6**. SADABS and SAINT the program were used.¹ All structures were solved by direct methods by using the SHELXS program of the SHELXTL package and refined with SHELXL.² Fig.s were generated by using Crystal-Maker.³ Further details were listed in Table S1 and Table S2.

3. CCDC numbers for complexes **1-6.**

CCDC 2350976-2350979 and 2350981-2350982 for complexes **1-6** contain the supplementary crystallographic data. These data can be obtained free of charge via <http://www.ccdc.cam.ac.uk/conts/retrieving.html>, or from the Cambridge Crystallographic Data Centre, 12 Union Road, Cambridge, CB2 1EZ, UK; fax: (+44) 1223-336-033; or e-mail: deposit@ccdc.cam.ac.uk.

4. Summary of crystallographic data for complexes 1-6.

Table S1. Summary of Crystallographic Data for Complexes 1-3

	1	2	3
chemical formula	C ₂₉ H ₂₄ N ₆ O ₈ Co	C ₂₉ H ₂₄ N ₆ O ₈ Zn	C ₆₂ H ₅₆ N ₁₂ O ₁₆ Ni ₂
fw	643.47	649.91	1342.61
Cryst syst	Monoclinic	Monoclinic	Triclinic
space group	P2 ₁ /c	P2 ₁ /c	P $\bar{1}$
<i>a</i> /Å	15.662(1)	15.603(1)	7.842(4)
<i>b</i> /Å	8.770(5)	8.651(8)	11.923(6)
<i>c</i> /Å	20.845(1)	20.841(1)	16.445(9)
α /deg	90	90	89.7(1)
β /deg	99.8(1)	101.0(1)	87.6(1)
γ /deg	90	90	73.4(1)
<i>V</i> /Å ³	2821.1(3)	2761.4(4)	1473.1(1)
<i>Z</i>	4	4	1
<i>D</i> _{calcd} , Mg/m ³	1.515	1.563	1.513
Abs coeff, mm ⁻¹	0.672	0.954	0.722
<i>F</i> (000)	1324	1336	696
Cryst size, mm	0.22 × 0.20 × 0.18	0.15 × 0.14 × 0.13	0.15 × 0.14 × 0.05
θ_{\min} , θ_{\max} , deg	1.98, 25.01	1.33, 25.01	1.24, 25.00
<i>T</i> /K	296(2)	296(2)	296(2)
no. of data collected	13997	13575	7389
no. of unique data	4979	4874	5101
no. of refined params	397	397	415
goodness-of-fit on <i>F</i> ² ^a	1.009	1.051	1.049
Final <i>R</i> indices ^b [<i>I</i> >2σ(<i>I</i>)]			
<i>R</i> ₁	0.0386	0.0297	0.0276
w <i>R</i> ₂	0.0916	0.0821	0.0693
<i>R</i> indices (all data)			
<i>R</i> ₁	0.0550	0.0356	0.0304
w <i>R</i> ₂	0.1028	0.0887	0.0720

^a Goof = [Σω($F_o^2 - F_c^2$)²/(*n-p*)]^{1/2}, where *n* is the number of reflection and *p* is the number of parameters refined. ^bR1 = Σ(| F_o | - | F_c |)/Σ| F_o |; wR2 = 1/[σ²(F_o^2) + (0.0691*P*) + 1.4100*P*] where *P* = ($F_o^2 + 2F_c^2$)/3.

Table S2. Summary of Crystallographic Data for Complexes 4-6

	4	5	6
chemical formula	C ₂₉ H ₂₄ N ₄ O ₆ SCu ·DMF	C ₃₂ H ₃₀ N ₄ O ₆ SCu ·CH ₃ OH	C ₃₆ H ₃ N ₄ O ₆₂ Co
fw	693.22	694.24	675.59
Cryst syst	Triclinic	Triclinic	Monoclinic
space group	<i>P</i> ī	<i>P</i> ī	<i>P</i> 2 ₁ /n
<i>a</i> /Å	10.546(8)	10.846(1)	11.126(1)
<i>b</i> /Å	12.516(9)	11.864(1)	14.273(1)
<i>c</i> /Å	12.968(9)	14.141(2)	19.771(1)
<i>α</i> /deg	68.8(1)	68.9(2)	90
<i>β</i> /deg	79.6(1)	72.7(2)	94.6(2)
<i>γ</i> /deg	72.3(1)	73.9(2)	90
<i>V</i> /Å ³	1517.1(1)	1591.7(4)	3129.9(5)
<i>Z</i>	2	2	4
<i>D</i> _{calcd} , Mg/m ³	1.518	1.449	1.434
Abs coeff, mm ⁻¹	0.847	0.806	0.603
<i>F</i> (000)	718	722	1404
Cryst size, mm	0.15 × 0.14 × 0.05	0.22 × 0.21 × 0.20	0.12 × 0.11 × 0.10
<i>θ</i> _{min} , <i>θ</i> _{max} , deg	1.69, 25.01	1.87, 25.01	2.03, 25.01
<i>T</i> /K	173(2)	296(2)	150(2)
no. of data collected	7667	8160	15616
no. of unique data	5301	5582	5497
no. of refined params	436	448	434
goodness-of-fit on <i>F</i> ² ^a	1.067	1.020	1.049
Final <i>R</i> indices ^b [<i>I</i> > 2σ(<i>I</i>)]			
<i>R</i> ₁	0.0983	0.0367	0.0289
<i>wR</i> ₂	0.2347	0.0941	0.0727
<i>R</i> indices (all data)			
<i>R</i> ₁	0.2223	0.0445	0.0328
<i>wR</i> ₂	0.2993	0.0994	0.0752

^a Goof = [Σω($F_o^2 - F_c^2$)²/(*n-p*)]^{1/2}, where *n* is the number of reflection and *p* is the number of parameters refined. ^bR1 = Σ(| F_o | - | F_c |)/Σ| F_o |; wR2 = 1/[$\sigma^2(F_o^2) + (0.0691P) + 1.4100P$] where *P* = ($F_o^2 + 2F_c^2$)/3.

5. The data of hydrogen bonds, π - π interactions and C-H \cdots π contacts of complexes 1-6.

Table S3. H-Bonding Geometry (\AA , $^\circ$) for complexes 1-3, 5 and 6

	D-H \cdots A	D-H	H \cdots A	D \cdots A	D-H \cdots A
1	C(15)-H(15A) \cdots O(5) ⁱ	0.969(3)	2.613(3)	3.068(4)	108.9(8)
2	C(15)-H(15A) \cdots O(5) ⁱ	0.970(2)	2.595(2)	3.002(3)	105.4(1)
3	C(17)-H(17A) \cdots O(8) ⁱ	0.970(1)	2.244(1)	3.202(2)	168.9(1)
	C(7)-H(7) \cdots O(5) ⁱⁱ	0.930(1)	2.644(1)	3.370(2)	135.3(1)
5	C(31)-H(31) \cdots O(5) ⁱ	0.930(3)	2.681(3)	3.523(5)	150.7(4)
6	C(21)-H(21) \cdots O(6) ⁱ	0.930	2.432(1)	3.124(2)	171.1(6)

Symmetry code: i: x , $-0.5 - y$, $0.5 + z$ for **1**. i: $-x$, $-y$, $1 - z$ for **2**. i: x , y , $-1+z$; ii: $1-x$, $2-y$, $1-z$ for **3**. i: $1 - x$, $1 - y$, $1 - z$ for **5**. i: $1 + x$, $2 + y$, z for **6**.

Table S4. Distances (\AA) of π - π interactions for 1-6

Complexes	π - π	
	face-to-face	center-to-center
1	3.394(3) (benzimidazole)	3.606(1) (benzimidazole)
	3.575(3) (benzimidazole)	3.594(2) (benzimidazole)
2	3.362(3) (benzimidazole)	3.483(3) (benzimidazole)
	3.353(3) (benzimidazole)	3.544(2) (benzimidazole)
3	3.437(2) (benzimidazole)	3.458(1) (benzimidazole)
4	3.330(1) (benzimidazole)	3.469(2) (benzimidazole)
5	3.742(4) (benzene)	4.376(4) (benzene)
6	3.412(2) (benzimidazole)	3.562(3) (benzimidazole)

6. The solid-state fluorescence spectra of L₁-L₃ and complexes 1-6

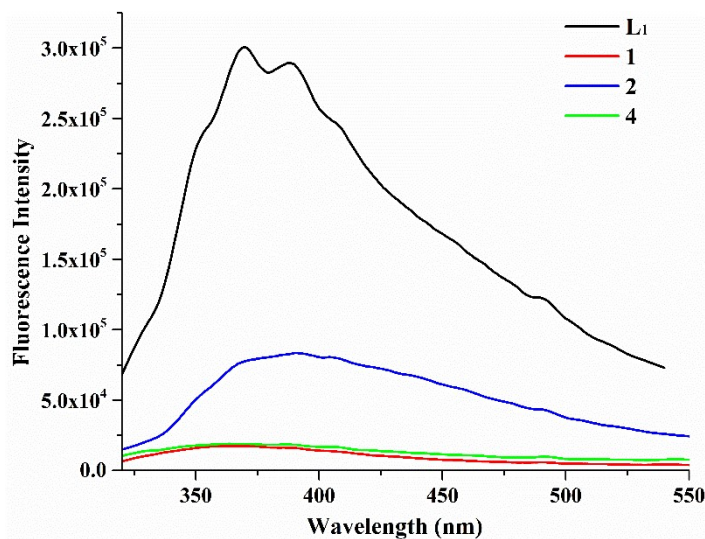


Fig. S1 The solid-state fluorescence spectra of L₁ and complexes **1**, **2** and **4** at room

temperature ($\lambda_{\text{ex}} = 300$ nm).

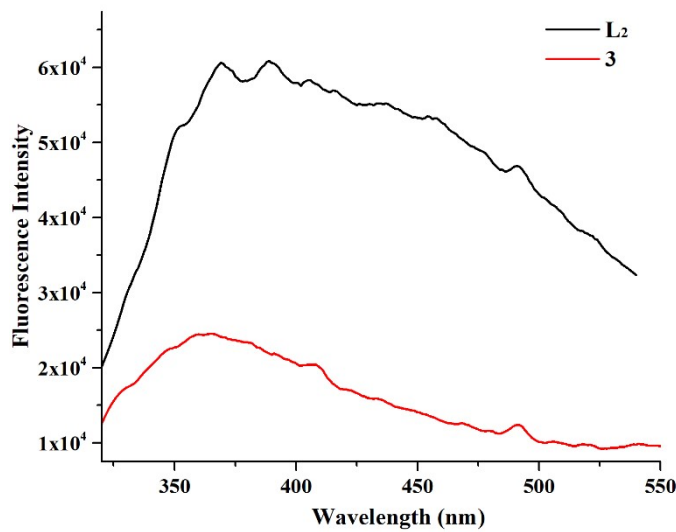


Fig. S2 The solid-state fluorescence spectra of \mathbf{L}_2 and complex $\mathbf{3}$ at room temperature ($\lambda_{\text{ex}} = 300$ nm).

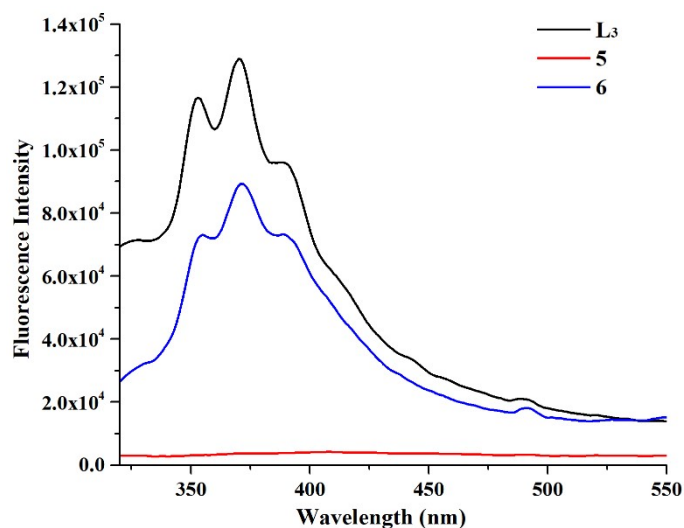


Fig. S3 The solid-state fluorescence spectra of \mathbf{L}_3 and complexes $\mathbf{5}$ and $\mathbf{6}$ at room temperature ($\lambda_{\text{ex}} = 300$ nm).

7. The simulated and experimental PXRD patterns for complexes 1-6

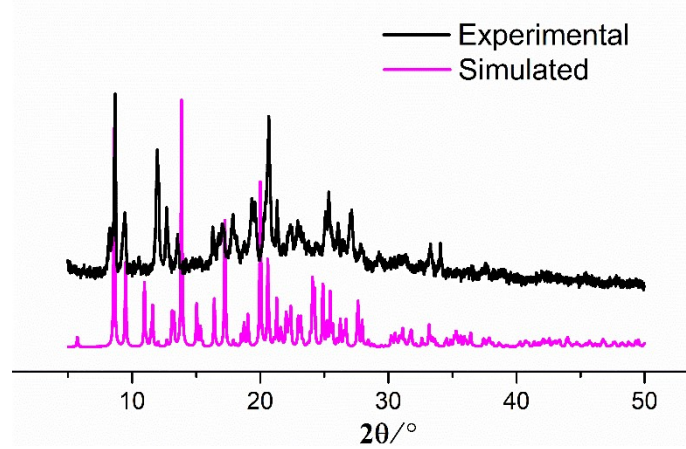


Fig. S4 The simulated (purple) and the experimental (black) PXRD patterns of **1**.

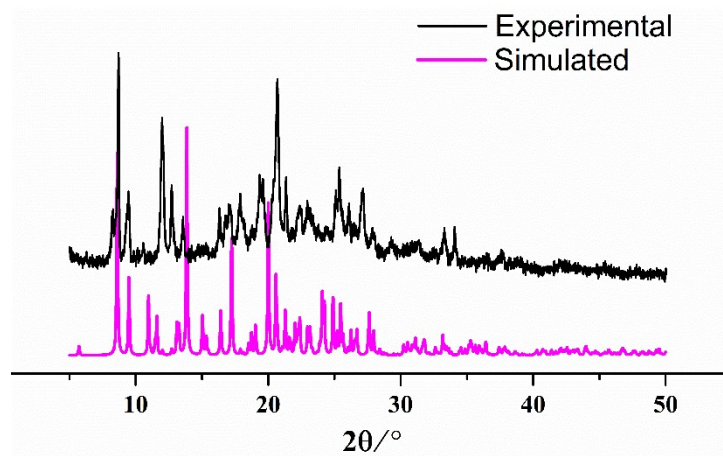


Fig. S5 The simulated (purple) and the experimental (black) PXRD patterns of **2**.

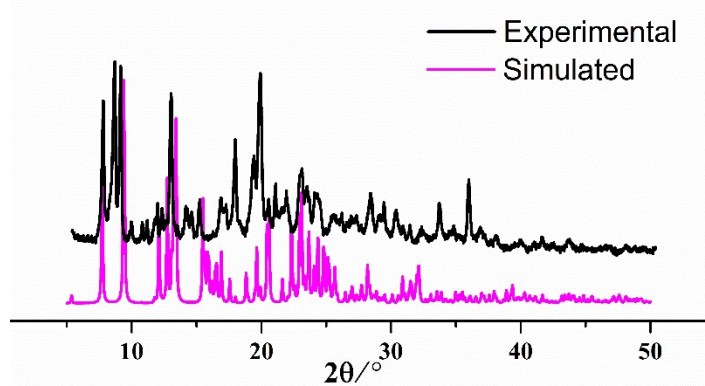


Fig. S6 The simulated (purple) and the experimental (black) PXRD patterns of **3**.

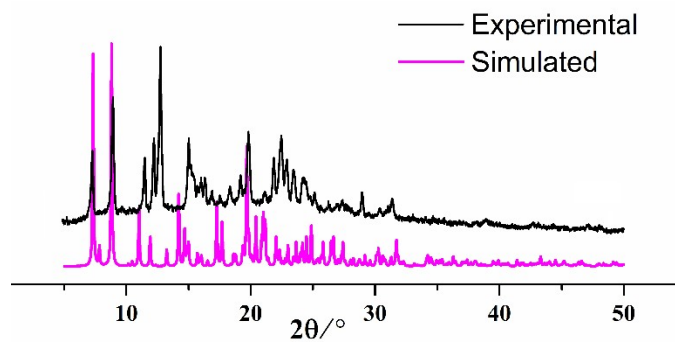


Fig. S7 The simulated (purple) and the experimental (black) PXRD patterns of **4**.

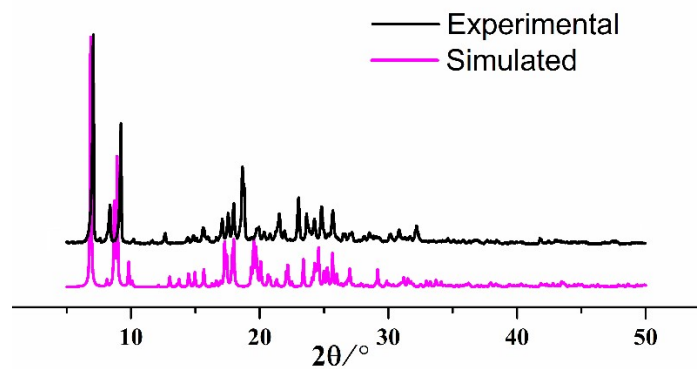


Fig. S8 The simulated (purple) and the experimental (black) PXRD patterns of **5**.

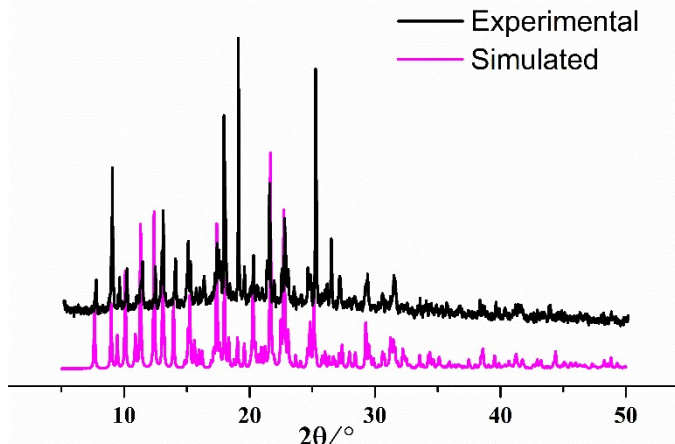


Fig. S9 The simulated (purple) and the experimental (black) PXRD patterns of **6**.

8. The curves of thermogravimetry for complexes 1-6

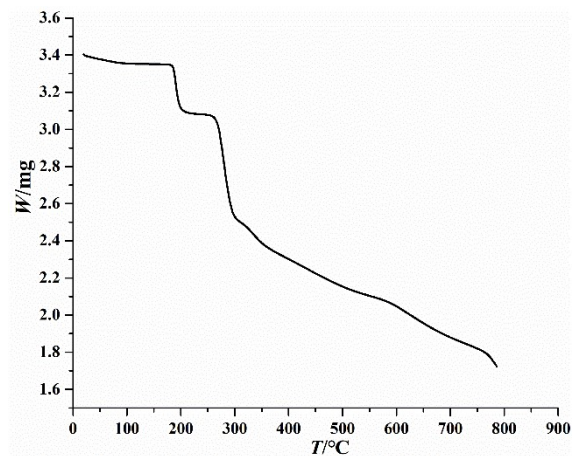


Fig. S10 TG curve from room temperature to 800 °C for **1**.

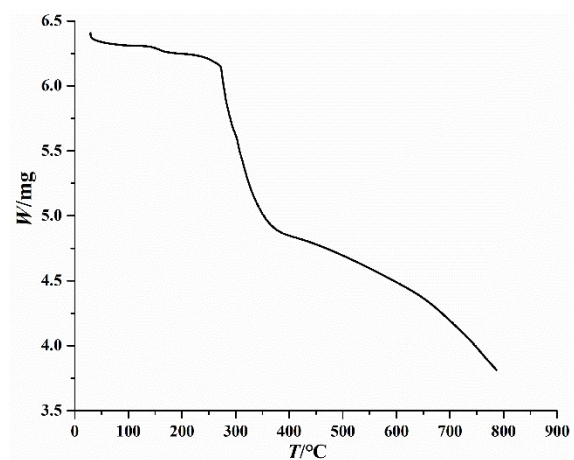


Fig. S11 TG curve from room temperature to 800 °C for **2**.

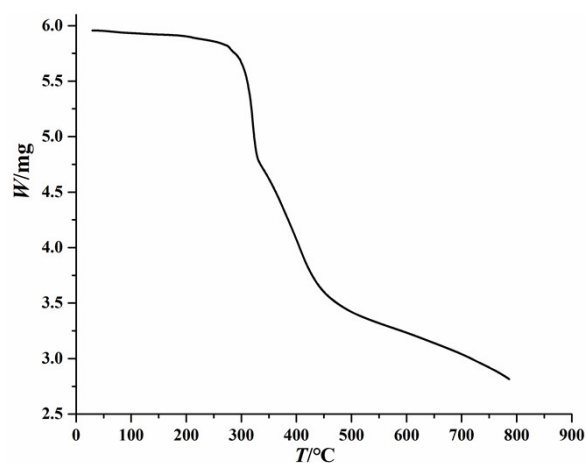


Fig. S12 TG curve from room temperature to 800 °C for **3**.

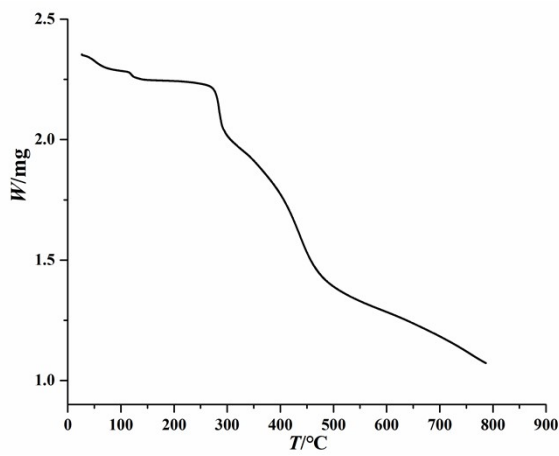


Fig. S13 TG curve from room temperature to 800 °C for 4.

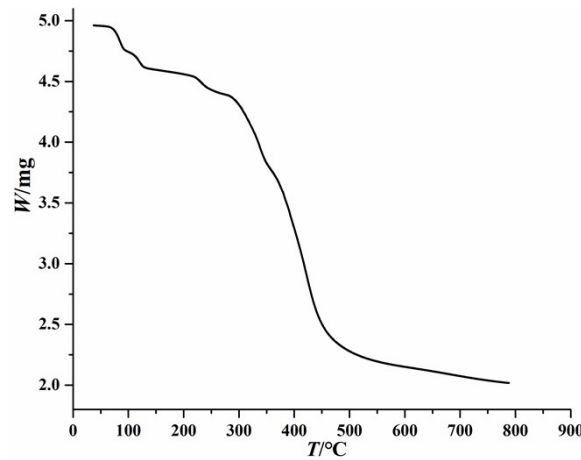


Fig. S14 TG curve from room temperature to 800 °C for 5.

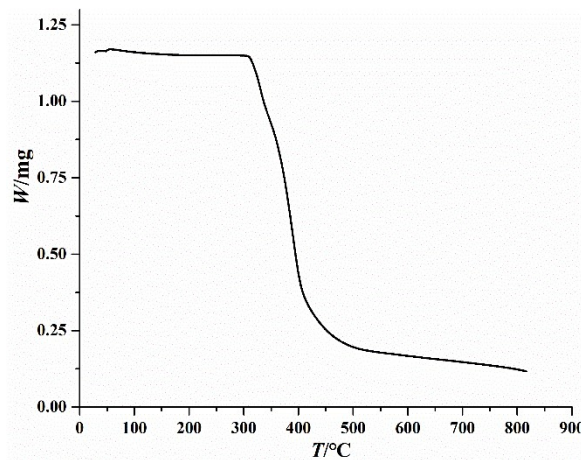


Fig. S15 TG curve from room temperature to 800 °C for 6.

9. The figures of fluorescence and UV-vis spectroscopies for complex 1.

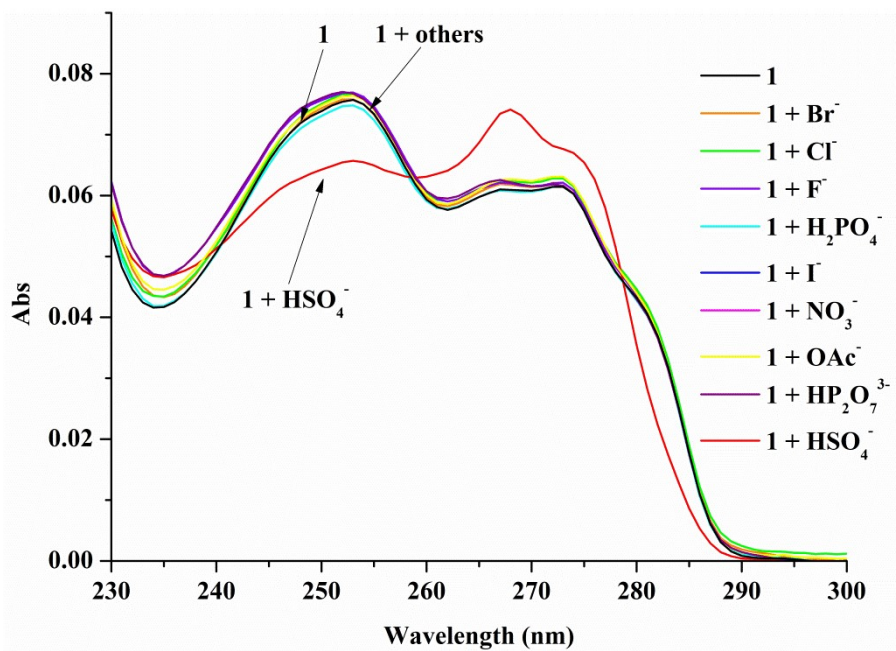


Fig. S16 UV/vis absorption spectra of **1** (5.0×10^{-6} mol/L) with salts (20.0 equiv.) of F^- , Cl^- , Br^- , I^- , H_2PO_4^- , OAc^- , NO_3^- , HSO_4^- , $\text{P}_2\text{O}_7^{2-}$ in $\text{CH}_3\text{CN}/\text{H}_2\text{O}$ (1:1, v/v) at room temperature.

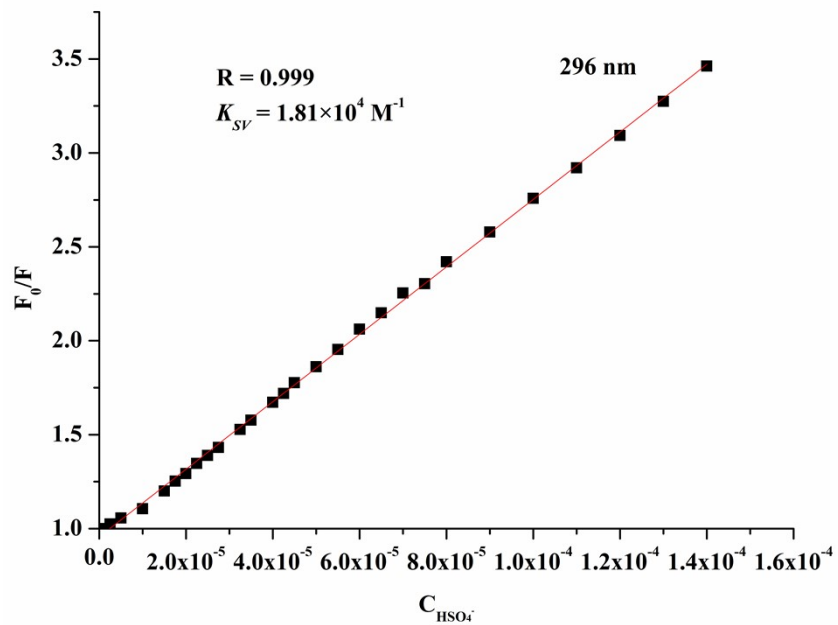


Fig. S17 Fluorescence titration fitting curve of complex **1** to HSO_4^- .

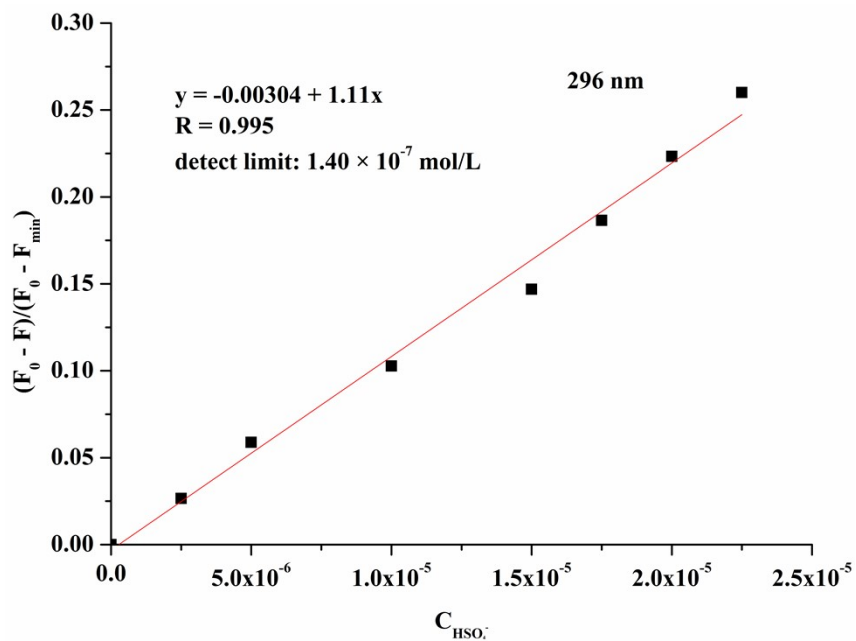


Fig. S18 Detection limit of complex **1** to HSO_4^- .

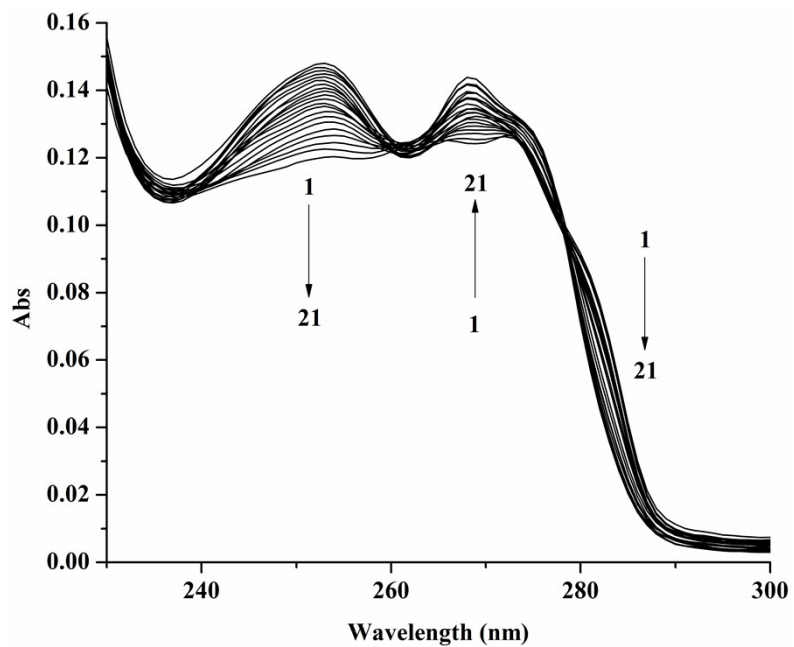


Fig. S19 UV/vis titration of **1** (5.0×10^{-6} mol/L) with diverse HSO_4^- in $\text{CH}_3\text{CN}/\text{H}_2\text{O}$ (v:v = 1:1) at room temperature. The concentrations of HSO_4^- are $0, 0.5, 1, 2, 3, 4, 5, 6, 7, 8, 9, 10, 11, 12, 14, 16, 18, 20, 25, 30, 35 \times 10^{-5}$ mol/L.

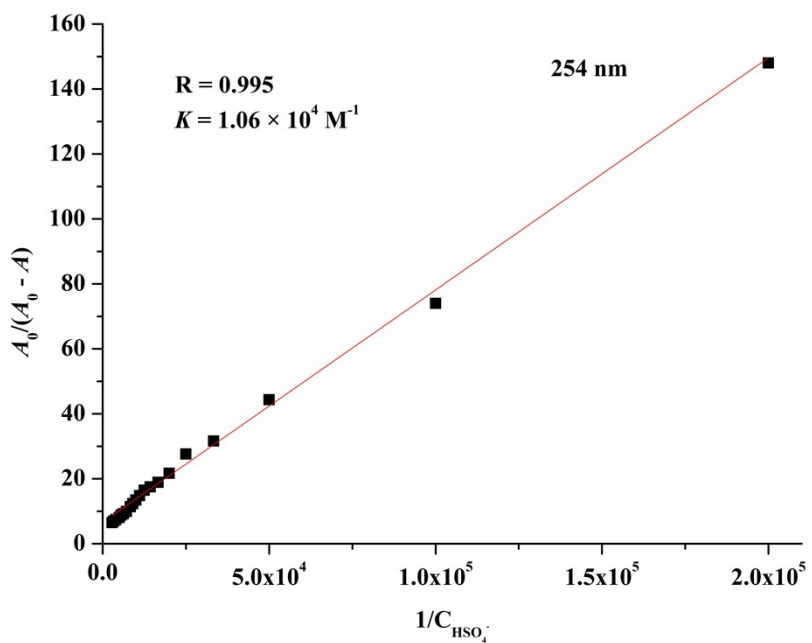


Fig. S20 UV titration fitting curve of complex **1** to HSO_4^- .

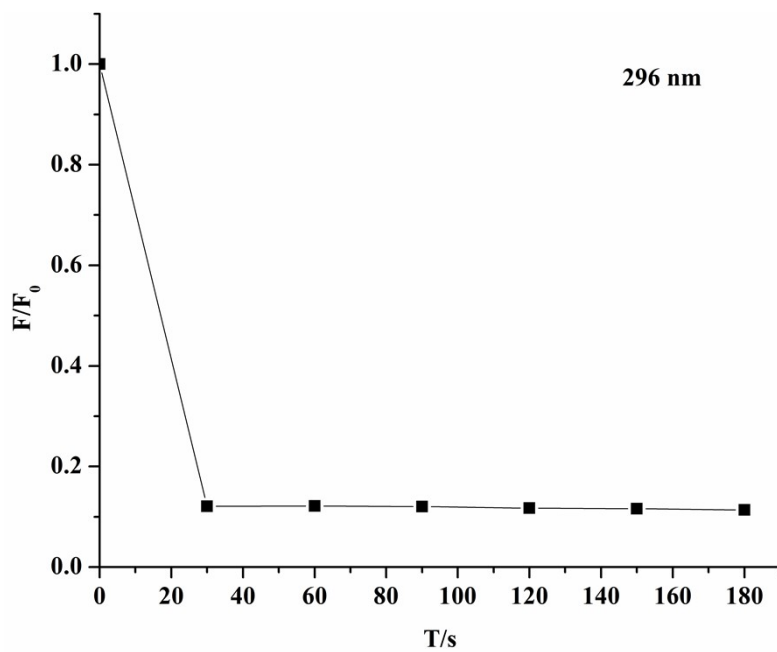


Fig. S21 Fluorescence response time of complex **1** to HSO_4^- .

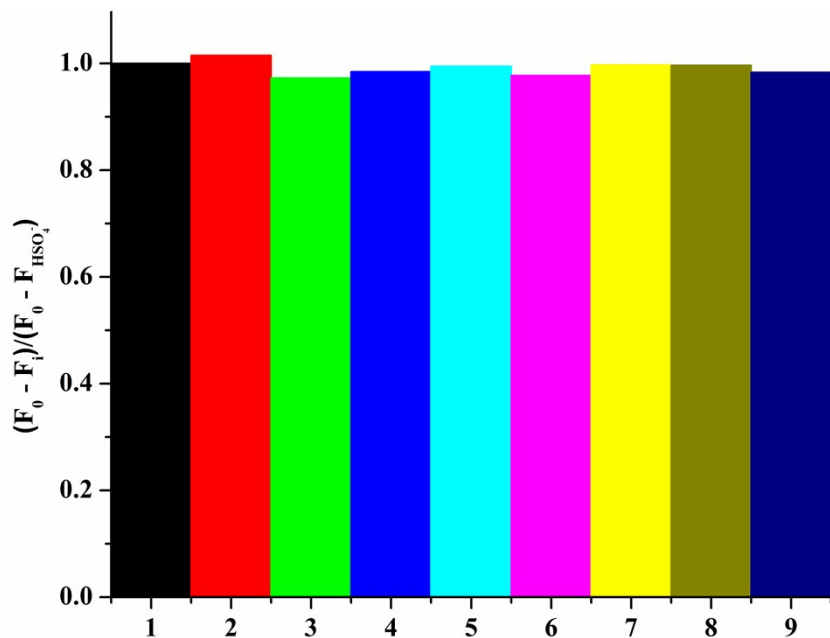


Fig. S22 Histogram of the interference of complex **1** with HSO₄⁻ at 296 nm (where the horizontal numbers represent the systems 1: **1** + HSO₄⁻; 2: **1** + HSO₄⁻ + F⁻; 3: **1** + HSO₄⁻ + Cl⁻; 4: **1** + HSO₄⁻ + Br⁻; 5: **1** + HSO₄⁻ + I⁻; 6: **1** + HSO₄⁻ + H₂PO₄⁻; 7: **1** + HSO₄⁻ + OAc⁻; 8: **1** + HSO₄⁻ + NO₃⁻; 9: **1** + HSO₄⁻ + HP₂O₇³⁻).

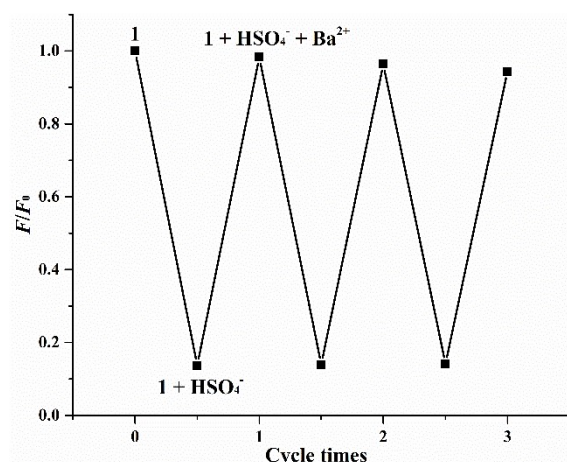


Fig. 23 Reversibility study of complex **1** (5×10^{-6} mol/L) for HSO₄⁻ (1.0×10^{-4} mol/L) in CH₃CN/H₂O (v/v = 1:1) at 296 nm at room temperature.

10. The Fig. of HRMS for **1** and **1**·HSO₄⁻

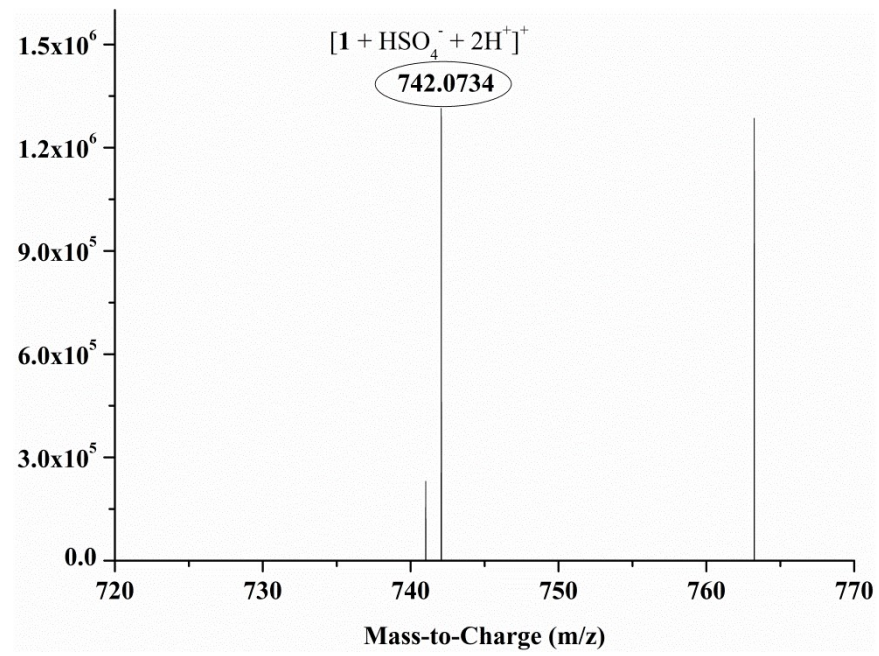


Fig. S24 HRMS of $\mathbf{1}\cdot\text{HSO}_4^-$.

11. Infrared spectra of **1** and $\mathbf{1}\cdot\text{HSO}_4^-$

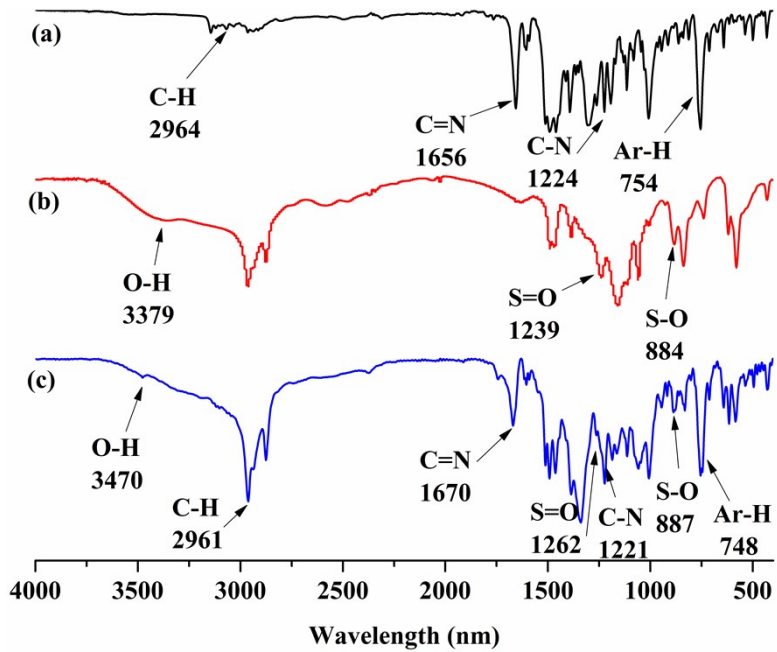


Fig. S25 (a) Infrared image of complex **1**; (b) Infrared image of HSO_4^- ; (c) Infrared image of $\mathbf{1}\cdot\text{HSO}_4^-$

References

S1 AXS, SAINT Software Reference Manual; Bruker: Madison, WI, 1998.

S2 G. M. Sheldrick, SHELXTL NT (Version 5.1), Program for Solution and

Refinement of Crystal Structures, University of Göttingen, Göttingen (Germany),
1997.

S3 D. C. Palmer, Crystal Maker 7.1.5, CrystalMaker Software: Yarnton, UK, 2006.